Title

Experimental Soil Warming and Permafrost Thaw Increase CH4 Emissions in an Upland Tundra Ecosystem

Journal
Journal of Geophysical Research Biogeosciences, 126(11)

ISSN
2169-8953

Authors
Taylor, MA
Celis, G
Ledman, JD
et al.

Publication Date
2021-11-01

DOI
10.1029/2021jg006376

Peer reviewed

Experimental soil warming and permafrost thaw increase CH_4 emissions in an upland tundra ecosystem

M.A. Taylor[1], G. Celis[2], J.D. Ledman[3, 4], M. Mauritz[5], S.M. Natali[6], E.–F. Pegoraro[7], C., Schädel[3], and E.A.G. Schuur[3]

[1]Yale School of the Environment, Yale University, New Haven, CT, USA

[2]Agronomy Department, University of Florida, Gainesville, Florida, USA.

[3] Center for Ecosystem Society and Science (ECOSS), Northern Arizona University, Flagstaff, Arizona, USA

[4] Bonanza Creek Long Term Ecological Research Site, University of Alaska, Fairbanks, AK, USA

[5] Biological Sciences, University of Texas at El Paso, El Paso, Texas, USA

[6] Woods Hole Research Center, Falmouth, MA, USA

[7]Climate Sciences Department, Climate and Ecosystem Sciences Division, Lawrence Berkeley National Laboratory, Berkeley, CA, USA.

Corresponding author: meghan.taylor@yale.edu,

phone: 313–550–5357

Key points:

1. Hotspots accounted for 72% of growing season methane emissions in a wet year in patches where sedges dominated the plant community.

2. Thawed soil volume was a strong driver of increased methane emissions, even in the absence of high surface moisture.

3. Increased methane emissions with deep thaw reduced net growing season carbon uptake by 18% in wet areas, and 4% in drier areas.

Abstract

Rapid Arctic warming is causing permafrost to thaw and exposing large quantities of soil organic carbon (C) to potential decomposition. In dry upland tundra systems, subsidence from thawing permafrost can increase surface soil moisture resulting in higher methane (CH_4) emissions from newly waterlogged soils. The proportion of C released as carbon dioxide (CO_2) and CH_4 remains uncertain as previously dry landscapes transition to a thawed state, resulting in both wetter and drier microsites.

To address how thaw and moisture interact to affect total C emissions, we measured CH_4 and CO_2 emissions from paired chambers across thaw and moisture gradients created by nine years of experimental soil warming in interior Alaska. Cumulative growing season (May – September) CH_4 emissions were elevated at both wetter (216.1 – 1099.4 mg CH_4-C m^{-2}) and drier (129.7 – 392.3 mg CH_4-C m^{-2}) deeply thawed microsites relative to shallow thaw (55.6 – 215.7 mg CH_4-C m^{-2}) and increased with higher deep soil temperatures and permafrost thaw depth. Interannual variability in CH_4 emissions was driven by wet conditions in graminoid dominated plots that generated >70% of emissions in a wet year. Shoulder season emissions were equivalent to growing season CH_4 emissions rates in the deeply thawed, warmed soils, highlighting the importance of non–growing season CH_4 emissions. Net C sink potential was reduced in deeply thawed wet plots by 4 – 42%, and by 3.5 – 8% in deeply thawed drier plots due to anaerobic respiration, suggesting that some dry upland tundra landscapes may transition into stronger CH_4 sources in a warming Arctic.

Plain Language Summary

The Arctic is warming twice as fast as the global average. This is causing permafrost to thaw and subside. Soil carbon decomposition under these conditions can be released as carbon dioxide in dry soils, or as methane in newly waterlogged soils, which has a stronger global warming potential. We artificially warmed permafrost soils to measure how thaw and moisture affects total carbon emissions in a dry, upland tundra ecosystem. Methane emissions were higher with deeper thaw and wetter soils, especially in plots with sedge tussocks. Permafrost thaw increased soil moisture and we expect that this will lead to increased methane emissions from even dry landscapes in future.

1. Introduction

With rising atmospheric temperatures in the Arctic, a significant proportion of the estimated 1440 – 1600 Pg soil organic carbon (C) stored in permafrost regions is exposed to potential decomposition as permafrost thaws (Hugelius et al., 2014; Overland et al., 2018; Schuur et al., 2018; Tarnocai et al., 2009). Decomposition of permafrost soil organic C may increase greenhouse gas (GHG) emissions to the atmosphere, accelerating global warming (Hugelius et al., 2014; Koven et al., 2011; Schaefer et al., 2011; Schuur et al., 2015). Some proportion of GHG emissions may be offset by increased plant growth, but C models and *in situ* studies indicate that on an annual basis, northern latitude systems will transition from a C sink to a source by 2100 (Belshe et al., 2013a; Koven et al., 2015; Lawrence et al., 2015; McGuire et al., 2018; Schuur et al., 2015).

Estimating the strength of the permafrost C–climate feedback is challenging, in part, because the form of GHG, carbon dioxide (CO_2) or methane (CH_4), that will be released as permafrost thaws is unclear. Determining the relative proportion of GHG emissions released as either CO_2 or CH_4 is crucial because CH_4 emissions have 45 times the sustained emissions global warming potential of CO_2 over a 100–year timescale, and may therefore have a significant effect on the GHG warming potential from high latitude terrestrial ecosystems (Neubauer and Megonigal, 2019).

A key environmental driver of the magnitude and form of C emissions is soil moisture (Humphrey et al., 2021). Permafrost acts as a barrier to vertical water flow, resulting in a perched water table and saturated conditions in the lower layers of the seasonally–thawed active layer (Walvoord and Kurylyk, 2016). As permafrost thaw deepens, soil moisture can change as a result of land subsidence (thermokarst) caused by loss of ground ice (Olefeldt et al., 2016), or soil drainage as ground water flow pathways increase (Lawrence et al., 2015). At the same time, climate change can alter the amount and seasonality of precipitation that also affects water flow and storage in permafrost ecosystems (Lique et al., 2016; Wrona et al., 2016).

The loss of ground ice in thawing permafrost is lacking in process–based Earth system models (Schädel et al., 2018). Though some manipulation studies have measured the effects of snow cover changes (Blanc–Betes et al., 2016) or water table changes (Vaughn et al., 2016) on GHG production and emissions, there are few direct observations of the effects of subsidence on C dynamics in tundra systems (Natali et al., 2015; Voigt et al., 2017). Even relatively dry, upland sites can become significant CH_4

sources with increasing thermokarst features across the landscape (Belshe et al., 2013b; Natali et al., 2015; Nauta et al., 2015; Taylor et al., 2018).

Terrestrial CH_4 emissions are spatially and temporally heterogeneous and mediated by changes in soil moisture and vegetation composition. These factors make emissions difficult to estimate across the Arctic (Lawrence et al., 2015; Nauta et al., 2015; Olefeldt et al., 2013; Olefeldt et al., 2016). Methane emissions are controlled by rates of production and oxidation within the soil column (Chowdhury et al., 2015; Dean et al., 2018). Production rates may be limited by absence of anaerobic microbial communities, substrate limitation, and anaerobic microsites in drier soils. In drier soils, diffusion of CH_4 through oxic soils above the water table can oxidize the majority of CH_4 produced before it reaches the soil surface (Preuss et al., 2013; Whalen, 2005). However, in tussock tundra, CH_4 can bypass oxic surface soils via rapid transport through the roots and stems of vascular plants (Andresen et al., 2017; Davidson et al., 2016; King et al., 1998; McEwing et al., 2015).

The Carbon in Permafrost Experimental Heating Research (CiPEHR) is a permafrost warming experiment initialized in 2008 (Natali et al., 2011). Within the footprint of CiPEHR, a water table manipulation experiment (DryPEHR) was established in 2011 to investigate the combined effects of thaw and water table change (Natali et al., 2015). In the first 3 years of warming, initial trends reflected the amplification of the C cycle, where a significant increase in CO_2 release was offset by C gains in enhanced plant productivity (Natali et al., 2011; Natali et al., 2014). However, there was significant variation in the C cycling response that was driven by heterogeneity in soil moisture. As thaw progressed, saturated sites had lower rates of gross primary productivity (GPP) and ecosystem respiration (R_{eco}), while well–drained, drier microsites had higher rates of R_{eco} and GPP (Mauritz et al., 2017; Natali et al., 2015). Previous measurements at the end of the growing season demonstrated this dry upland site had net CH_4 emissions from both warmed and ambient plots, and that CH_4 emissions were positively related to soil moisture (Natali et al., 2015). However, these CH_4 measurements were only collected once at the end of the growing season and did not represent CH_4 throughout the growing season and its contribution to the net ecosystem C balance. Moreover, site-level water content has increased significantly relatively to 2011, and thermokarst features have become more prevalent on the landscape (Pegoraro et al., 2020).

Our objectives in this study were to collect paired chamber CH_4 and CO_2 exchange measurements throughout several growing seasons to directly quantify the growing season C budget in response to accelerated soil warming, thaw, and subsidence. We hypothesized that: 1) Soil moisture would be the most important driver of CH_4 emissions in this upland tundra ecosystem; and 2) Cumulative C emissions at the ecosystem scale would be greatest in well–drained and deeply thawed plots due to higher rates of aerobic respiration leading to larger CO_2 emissions.

2. Methods

Site Description

The Carbon in Permafrost Experimental Heating Research (CiPEHR) experiment is located within the Eight Mile Lake watershed (63˚52’42”N, 149˚13’12”W), in the northern foothills of the Alaska Range near Denali National Park and Preserve. The study site is located at 700 m elevation on a gentle hill slope (~5%) (Belshe et al., 2013b).

Surface soils are relatively well–drained and consist of 0.25 – 0.35 m deep organic soils overlying mineral soil made up of glacial till and loess deposits (Osterkamp et al., 2009; Schuur et al., 2009; Vogel et al., 2009). The upland tundra vegetation forms an open canopy and is dominated by low, dwarf shrubs (e.g.: *Betula nana*, *Vaccinium uliginosum*), tussock forming sedges (*Eriophorum vaginatum*), and mosses and lichen (Natali et al., 2012; Salmon et al., 2016; Schuur et al., 2007; Walker et al., 2005). While it falls within the discontinuous permafrost zone, this site entirely underlain with permafrost (Osterkamp et al., 2009), and the site is co–located with a 30 m deep borehole where permafrost warming has been recorded since 1985 (Osterkamp and Romanovsky, 1999). Soils have an average of 54.8% moisture by mass, and ice loss drives 85-91% of subsidence at this site (Rodenhizer et al., 2020).

Experimental design

The CiPEHR experiment was established in 2008 when maximum active layer thickness (ALT) was at 50 cm depth (Natali et al., 2011). Permafrost warming was achieved using snow fences (1.5 m x 8 m) that trap excess snow, insulating permafrost and increasing soil temperatures by 2 – 3 ˚C during winter months (Mauritz et al., 2017; Natali et al., 2011). In spring of each year, immediately prior to snowmelt, the excess snow pack was removed to ambient levels to prevent excess moisture and to ensure similar melt–out dates between treatments. There are six replicate fences within 3 experimental blocks that are located in close proximity (100 m) of each other. Within each block are 8 plots (0.6 m x 0.6 m). Air warming treatments were applied to two plots on each side of the fence (soil warming on one side, control on the other) using 0.36 m^2 x 0.5 m tall open top chambers during the growing season (May – September).

A water table drawdown experiment (DryPEHR) was initiated in the footprint of the snow fences in June 2011 to examine the effects of thaw and soil moisture changes (Natali et al., 2015). However, permafrost thaw and changing microtopography that underlay the water table manipulations have also altered the hydrology and helped to produce the final set of plot conditions (Figure S1). As a result, we have reclassified wet and dry microsites within the thawing experiment as described below.

Plot groupings based on water table depth and thaw depth

Heterogeneous thaw conditions across CiPEHR and DryPEHR plots have led to increasingly variable thaw and soil moisture conditions across treatments ranging from standing water (wet) to deep (dry) WTDs. Therefore, we classified plots into 3 groups based on active layer thickness and mean WTD in 2017 following Mauritz et al. (2019): Shallow–Dry (average WTD –17.6 cm; average maximum thaw depth 76.3 cm; n = 22), Deep–Dry (average WTD –14.4 cm; average maximum thaw depth 112.5 cm; n = 8) and Deep–Wet (average WTD –1.0 cm; average maximum thaw depth 115.7 cm; n = 12) (Figure S1). Deeply thawed plots were part of the soil warming treatment. The Shallow-Dry group were not warmed and are closest to ambient tundra thaw and soil moisture. These groups were not used for statistical analyses, which were conducted on continuous plot variables. Groups were used to visualize the averaged plot conditions that capture potential future tundra trajectories.

Environmental variables

Meteorological conditions were monitored half–hourly using a HOBO Onset station (Bourne, MA, USA) located between the three experimental blocks. The station measured air temperature, rainfall, photosynthetically active radiation (PAR), wind speed and direction, and relative humidity. Soil temperatures were measured half–hourly at 5, 10, 20, and 40 cm depth in every flux plot using type T copper–constantan thermocouples. Volumetric water content (VWC) was measured in every flux plot from the soil surface to 20 cm depth using site–calibrated water content reflectometer probes (Campbell CS 615 and CS616). All plot level measurements were recorded to a data logger (CR1000, Logan, UT). Water table depth (WTD) was measured three times per week in wells adjacent to plots and thaw depth was measured once per week at two locations surrounding each plot during the snow–free period. Water table depth is reported relative to the ground surface: negative values reflect water below the soil surface and positive numbers reflect water above the soil surface.

Aboveground biomass measurement

We quantified plant species composition and biomass at CO_2 flux plots in late July, 2017, at the peak of the growing season, using a non–destructive point intercept method (Schuur et al., 2007). A 60 x 60 cm frame with 49 grid points was suspended over the CO_2 flux plots. A rod was lowered into the vegetation at each grid point and the species at each point of contact was recorded. Based upon species–specific allometries from the site, the average number of contact points per species was converted to dry weight biomass (g/m^2) (Salmon et al., 2016). The same technique was used to estimate biomass at the CH_4 flux plots, but these plots were smaller so only grid points that fell within the collars were used (between 9–13 points per collar).

Methane flux measurements

Methane flux measurements were made at collars adjacent to CO_2 flux plots (n = 21) within the same plot footprint. Collars are made of 25 cm PVC that were permanently installed 8 cm into the soil layer. Surface flux measurements were made with a Los Gatos Research (LGR), Ultra–Portable Methane Analyzer (UMA), (Model number 915–0001, Los Gatos, Research, Palo Alto, CA, USA). The LGR was checked against a CH_4 standard and atmospheric concentrations to ensure good agreement during each measurement date. We covered the collars with an opaque 10 L chamber that fits tightly over the collar and makes an air tight seal and recirculated air between the UMA and chamber via inlet and outlet tubing for 15 minutes. Between separate plots, the chamber was removed until CH_4 values returned to background atmospheric levels. Methane fluxes were calculated using a linear slope fitting technique of 5 minutes of the measured data. Non–zero fluxes with $r^2 < 75\%$ were discarded (3.5% of all measurements); fluxes that were not significantly different from zero were retained irrespective of r^2 values.

In 2016, measurements were made 12 times in late summer and into the shoulder season (August 8th – November 14th). In 2017 and 2018 measurements were made throughout the growing season from May 4 – September 4 in 2017 (9 times) and May 25th – August 29th in 2018 (8 times). Measurements began later in the 2018 growing season due to late snowmelt across the site.

Carbon dioxide flux measurements

Net ecosystem exchange (NEE) was measured using an automated CO_2 flux chamber system from May 1 until the end of September, from 2016 to 2018. Measurements were made every 1.5 h where air was circulated between the chambers and an infrared gas analyzer (IRGA; LI–820, LICOR Corp., Lincoln, Nebraska) for 1.5 min, and CO_2 concentrations were measured at 2 s intervals. Plot level air temperatures were measured every 1.5 hours using shaded thermistors from inside the autochambers during CO_2 flux measurements when chambers were closed and fans circulated air inside the chamber. Fluxes were calculated using linear regression, and converted from volume to mass using plot-specific chamber volumes and air temperatures. Ecosystem respiration was modeled with soil temperatures at 10 cm using an exponential Arrhenius-type equation (Mauritz et al., 2017; Natali et al., 2014; Natali et al., 2011). This temperature relationship was used to estimate R_{eco} when photosynthetically active radiation (PAR) < 5 μmol m^2 s^{-1}. When PAR > 5 μmol m^2 s^{-1}, NEE was gap filled using a hyperbolic light response curve. Gross primary productivity was estimated when PAR ≥ μmol m^2 s^{-1} where GPP = NEE + R_{eco}. More details on the flux system and calculations can be found in Mauritz et al., (2017), Natali et al., (2011), Natali et al., (2014), and Vogel et al., (2009).

Fall flux measurements were made from October – November 2016, after summer auto–chambers were removed. Fluxes were measured following Webb et al., (2016), by circulating air through a plexi-glass chamber (108 L average volume) and an infrared gas analyzer. Light and dark flux measurements were made using a dark chamber cover in order to estimate NEE and R_{eco}, respectively.

Cumulative greenhouse gas emissions

Cumulative seasonal CH_4 emissions for the 2017 – 2018 growing seasons (May – September) and 2016 end of summer/shoulder season (August – November) were calculated by linearly interpolating between measurement periods and summing fluxes at each plot. Cumulative CO_2 fluxes were calculated from half–hourly flux rates and reported in g CO_2-C m^{-2} following Mauritz et al., (2017). We use the convention that positive NEE values represent a net CO_2 sink, and negative NEE values represent a net CO_2 source. Cumulative fall season fluxes were interpolated and summed using the following shoulder–season exponential equation ($r^2 = 0.27$; $Q_{10} = 1.89$) based upon the relationship between R_{eco}, soil temperature (5 cm), and day of year (DOY) (Webb et al., 2016):

$$NEE = a * e^{\wedge} (b * T_{5cm} + c * DOY)$$

Where a = 1938.6; b = 0.06, and c = -0.03. During the shoulder season, NEE is equivalent to R_{eco}.

Methane emissions are reported in mg CH_4-C. In order to compare the relative radiative impacts of CO_2 and CH_4, we calculated the CO_2 equivalent of CH_4. We chose to use the sustained global warming potential (SGWP) metric because these fluxes are radiative forcing due to sustained emissions as opposed to pulse emissions (Neubauer & Megonigal, 2019). Here we are using the 100-year SGWP of 45 that was reported on a mass of gas basis, while accounting for the different molar gas masses of CH_4 (16 g mol^{-1}) and CO_2 (44 g mol^{-1}). This gives 16.4 as a multiplier to present CH_4 and CO_2 data on an equivalent basis (Neubauer & Megonigal, 2019):

$$CO_2\text{-equivalent} = F \times SGWP$$

Where F = cumulative CH_4 flux (mg CH_4-C); SGWP is 16.4 (=(16 g mol^{-1}/44 g mol^{-1})*45), the mass-adjusted 100 year sustained global warming potential. For example, the release of -215.7 mg CH_4-C is equivalent in radiative forcing to the release of -3.5 g CO_2-C based on the 100 year sustained global warming potential ((-215.7 mg) * (0.001 mg^{-1}g) * (16.4) = -3.5 g CO_2-C-equivalent greenhouse gas emission.

We use an ecosystem-based sign convention here, where cumulative CH_4 emissions will be denoted as positive when it is a net sink and negative when a net source of CH_4. When cumulative NEE is positive, that shows net CO_2-C sink, when it is negative that means net CO_2-C source.

Statistical analyses

To determine drivers of CH_4 emissions at each plot during the growing seasons in 2017 and 2018 we used mixed effects models (lme4, Pinheiro et al., 2017) in R (R Core Team, 2018). The 2016 growing season was not modeled because measurements did not begin until late July. Mean weekly thaw depth, WTD, deep (20 – 40 cm) soil temperatures, and shallow (5 – 10) soil temperatures were included as fixed effects and all interactions were allowed. Plot was included as a random effect to account for repeated measures. We included plant biomass as a random effect to account for variability among plots, but it did not improve model fit and so it was removed. Methane was log transformed to achieve normality before analyses. Correlation among environmental variables was tested using a variable inflation factor (VIF) test and variables were standardized to compare effect sizes. The significance of the fixed effects was assessed by calculating 95% confidence intervals for model coefficients using bootstrapping techniques. The best models were selected using stepwise backward selection where individual variables were removed and compared to the full model using Akaike Information Criterion (AIC). The best fitting, simplest model was selected using a 5–point AIC improvement (Pinheiro and Bates, 2000; Zuur et al., 2009). Shallow soil temperatures did not improve model fit and were removed from the model. To test for significant effects between the plot groupings based on mean WTD and maximum thaw depth and years, we used one–way ANOVA (package emmeans, Lenth, 2019) and a *t*–test.

3. Results

Environmental variables

Growing season mean annual air temperatures were similar across all years of measurement, ranging from 9.7 – 10.4˚C (Table 1). Insulation from the snowpack warmed surface soils by an average of 0.4 ˚C and deep soils by 1.0˚C relative to control during the 2016 – 2018 growing seasons. The site was snow free before May 1st in 2016 and 2017, while in 2018 the onset of the growing season was delayed as snow remained until after May 10th. Active layer thickness in warmed permafrost soils was 39 cm deeper than control plots across 2016 – 2018 on average.

Soils began to thaw 2 weeks earlier in 2017 relative to 2016 and 2018. There was evidence that a talik ((i.e., an area of unfrozen ground surrounded by permafrost and frozen surface soil in the winter) was present in soil warmed plots in 2016 and 2018. When the talik depth was reached, thaw depth in soil–warmed plots diverged rapidly from control (Figure 1C, D). In contrast, in 2017, the entire column refroze, and thaw progressed linearly through the whole season (Figure 1C, D). Refreezing in 2017 is likely related to the very late snowfall onset in winter 2016/2017, which allowed cold air temperature to fully refreeze the soil column (Figure S2).

Growing season precipitation was above long–term average in 2016, and rainfall in July exceeded the 10-year average for that month at this site. Precipitation in 2017 was just below average and fell primarily in July and August (Figure 1A). In 2018, precipitation was above average and was concentrated (60%) towards the end of the growing season, after August 20th (Figure 1A; Table 1). As a result of increased subsidence (Plaza et al., 2019; Rodenhizer et al., 2020), soil–warmed plots were wetter on average than control plots (WTD ~ 10 cm shallower/closer to the surface) from 2016 – 2018 (Table 1). Water table depth correlated strongly with precipitation at the site, and the timing of rainfall was reflected in seasonal WTD patterns (Figure 1A, B, C).

Plant species composition and biomass

Average total plant biomass measured in each CH_4 collar in summer 2017 was similar among groups (Shallow Dry: 440.9 ± 46.7 g m^{-2}; Deep Dry: 406.6 ± 107.3 g m^{-2}; Deep wet: 347.5 ± 55.8 g m^{-2}). Because graminoid vegetation have aerenchyma that can aid in CH_4 transport from soils to the atmosphere, we wanted to quantify the plot-level varation in *E. vaginatum* and *C. bigelowii*. We calculated graminoid species composition as a percentage of total biomass in each CH_4 collar and averaged them by groups. Percent graminoid species (*E. vaginatum* and *C. bigelowii*) was not significantly different between groups. Nine of the plots (n = 42) measured had > 30 % graminoid cover. Five of them were among the Shallow Dry group, 3 in the Deep Wet, and 1 in Deep Dry. Plant functional type composition summarized by groups can be found in Table S1.

Seasonal CH_4 emissions in response to environmental drivers

Methane emissions increased during the growing season, reaching a peak in late August in 2017, and in late July, 2018 (Figure 2A, B, C). Deep Wet mean daily flux rates reached -378 and -71 mg CH_4-C m^{-2} d^{-1} in August 2017 and 2018, respectively. Deep Dry fluxes reached -49 and -19 mg CH_4-C m^{-2} d^{-1} in August 2017 and 2018, respectively and Shallow Dry were -47 and -14 mg CH_4-C m^{-2} d^{-1} in August 2017 and 2018, respectively. In 2016, measurements spanned August – November, and Deep Wet, Deep Dry, and Shallow Dry all reached high mean daily flux rates of -655, -220, and -81 mg CH_4-C m^{-2}

d^{-1} in August. A small subset of plots consistently emitted more CH_4 in 2016 and 2017, but this was not seen in 2018 measurements (Figure 2A, B, C).

We analyzed weekly cumulative CH_4 emissions across all plots in 2017 and 2018 in response to changes in weekly mean thaw depth, water table depth, and deep soil temperatures (20 – 40 cm). In 2017, CH_4 emissions increased with thaw depth and shallower water table (wetter conditions) (Table 2). In 2018, CH_4 emissions increased with thaw depth and deep soil temperatures with a significant interaction between these two terms (Table 2). In deeply thawed plots, where we see the talik, thaw depths increased rapidly from < 20 to more than 70 cm within a week after May 27th (Figure 1C, D). In those plots the relationship between thaw depth and CH_4 emissions was decoupled as a result of the non–linear increase in thaw (Figure 3B) in contrast with Shallow Dry plots in 2018. In deeply thawed plots, higher CH_4 emissions are instead coupled with increasing deep soil temperatures (Figure 3D).

Cumulative CO_2 and CH_4 emissions

Cumulative CH_4 emissions were elevated in both Deep thaw groups relative to Shallow Dry, with large inter–annual variation in the magnitude of CH_4 emissions between 2017 where Deep Wet and Deep Dry plots emitted -934 and -390 mg CH_4-C m^{-2} d^{-1} versus 2018 where they emitted less than half of that, -216 and -130 mg CH_4-C m^{-2} d^{-1} respectively (Table 3; Figure 2). In 2016 where only August – November was measured, Deep Wet and Deep Dry plots had the highest cumulative emissions (-1099 and -392 mg CH_4-C m^{-2} d^{-1}), which suggests that the 2016 growing season likely saw high CH_4 emissions rates during the growing season relative to 2017 and 2018. In all years, Deep Wet plots experienced highest CH_4 emissions, followed by Deep Dry and then Shallow

Dry plots. In 2017, emissions from the Deep Wet plots were 12 times higher and Deep Dry plots were 2.5 times higher relative to Shallow Dry (Table 3). The same patterns held in 2018, but the overall magnitude of CH_4 emissions was much lower, especially for Deep Wet plots. In 2018, cumulative Deep Wet plot CH_4 emissions were 4 times higher than Shallow Dry, and 2 times higher than Deep Dry plots (Table 3).

Net ecosystem exchange (g CO_2-C m^{-2}) was positive, and therefore a net sink for all groups during this growing season time period. However, the sink strength was reduced in deeply thawed plots relation to shallow thaw. In 2016 measurements (August – September), NEE in Shallow Dry plots was similarly high, but in Deep Dry and Deep Wet plots, NEE was reduced by ~50% (Table 3) compared to 2017. In 2018, NEE was reduced in Shallow Dry and Deep Dry plots relative to previous years, while in Deep Wet plots, NEE was similar to 2017 (Table 3). Taking into account the SGWP of CH_4 for each group (CO_2-equivalence for the growing season), CH_4 emissions reduced net growing season C uptake by 18.2% in Deep Wet plots, by 4.3% in Deep Dry plots and 1.0% in Shallow Dry plots in 2017 (Table 3). In summer 2018, CH_4 emissions reduced net C uptake similarly between Deep Wet (4.4%) and Deep Dry plots (3.5%) (Table 3). There was less reduction of C uptake in Shallow Dry plots (0.9%) (Table 3).

Shoulder season NEE and CH_4 emissions were measured in 2016 in October and November. Shoulder season NEE was near net–neutral, and similar among Shallow Dry (–0.37 ± 0.003 g CO_2-C m^{-2}), Deep Dry (–0.39 ± 0.004 g CO_2-C m^{-2}), and Deep Wet (–0.39 ± 0.006 g CO_2-C m^{-2}) plots. In contrast, CH_4 emissions were remained high through October and began to taper off in November. Deep Wet emissions were highest (-58.73 ±

37.72 mg CH_4-C m^{-2}), and Deep Dry (-38.63 ± 11.97 mg CH_4-C m^{-2}) and Shallow Dry were similar (-35.20 ± 17.73 mg CH_4-C m^{-2}).

On an annual basis in total C, Shallow Dry plots range between a net C source (negative) or sink (positive) (–78 to 35 g C m^{-2} y^{-1}). Deeply thawed plots trended towards a net C source, where Deep Dry plots ranged between a stronger net C source or net neutral values (–102 to 1 g C m^{-2} y^{-1}), and Deep Wet plots are the strongest C source (–124 to –20 g C m^{-2} y^{-1}).

4. Discussion

Permafrost thaw can trigger significant changes in soil moisture that can create a high degree of landscape heterogeneity, affecting C dynamics. Under experimental soil warming of 1–2°C at this upland site, a 5x increase in subsidence was measured with commensurate changes to hydrology (Rodenhizer et al., 2020). Such changes in landscape moisture may make it more difficult to project short– and long–term changes in ecosystem C storage, due to the shifting balance of CO_2 versus CH_4 released from soils, the seasonality of fluxes, and the magnitude of plant C uptake. At CiPEHR, rapid thaw has led to development of both wetter and drier microsites due to heterogeneous patterns of subsidence. Loss of soil ice structures has caused soil surface slumping and brought the water table closer to or above the soil surface, especially when growing season precipitation is high (Mauritz et al., 2017; Plaza et al., 2019; Rodenhizer et al., 2020). In the short term, moisture affects plant productivity and the system's ability to offset C losses as permafrost thaws (Mauritz et al., 2017). Ecosystem C storage in deeply thawed upland tundra is significantly affected by thermokarst formation and higher soil moisture (Schuur and Mack, 2018). At CiPEHR, we have observed a faster decline in

GPP relative to R_{eco} in subsided sites (Mauritz et al., 2017). In addition to affecting plant uptake of C during the growing season, we show that increased soil moisture further impacts net C uptake by releasing significantly more CH_4, even in this upland system.

Environmental drivers of CH_4 emissions

During both full growing seasons measured, thaw depth emerged as an important variable driving increased CH_4 emission at CiPEHR. This strong relationship between seasonal fluxes and thaw depth may actually represent different dominant controls on CH_4 emissions where soil temperatures are important earlier in the season, while the volume of unfrozen soil is a more important factor late in the growing season as soil temperatures cool. The importance of thaw depth has been demonstrated at other Alaskan tundra studies that similarly found landscape level CH_4 emissions increased with increasing thaw depth (Sturtevant et al., 2012; Taylor et al., 2018; von Fischer et al., 2010; Zona et al., 2009; Zona et al., 2016). Thaw depth progresses with seasonally increasing soil temperature and represents the total volume of unfrozen soil and therefore the amount of organic matter available for methanogenesis (Sturtevant et al., 2012; Olefeldt et al., 2013; von Fisher et al., 2010; Zona et al., 2009; Voigt et al., 2019). Thaw depth integrates a combination of factors that directly or indirectly control CH_4 production and oxidation. While microbial metabolism should depend directly on temperature, the relationship between soil temperatures and CH_4 emissions is hysteretic in this upland tundra site (Taylor et al., 2018), which suggests that temperature alone cannot account for the complexity of environmental factors controlling CH_4 emissions.

The importance of thawed soil volume is demonstrated by the Shallow Dry and Deep Dry plots. In the absence of strong surface moisture changes, Deep Dry plots exhibited higher CH_4 emissions than Shallow Dry plots, where warmer growing season soil temperature and/or a more deeply thawed soil profile were sufficient to increase CH_4 emissions (Figure 3). However, the presence of taliks in warmed soils may ultimately result in decoupling of thaw depth from soil temperature and moisture. In 2018, taliks formed early in the growing season when soils were still quite cold, and so seasonal CH_4 emissions were more strongly tied to increasing soil temperature rather than thaw depth (Table 2). The presence of taliks would likely increase non–growing season CH_4 emissions as well because of the persistence of unfrozen soil. While we were not able to measure this directly at CiPEHR, landscape scale data covering a mosaic of permafrost thaw from the nearby eddy covariance tower at Eight Mile Lake suggests ongoing CH_4 production in deeper, unfrozen soils that released suddenly during warming events in early spring and mid–winter (Taylor et al., 2018). Methane outbursts from mid–winter warming events at Eight Mile Lake accounted for 1/3 of the annual CH_4 emissions in 2016/2017 (Taylor et al., 2018).

While thaw, soil temperature, and soil moisture explained most of the linear seasonal trends in CH_4 emissions, the overall magnitude of emissions in a given year was driven by a subset of plots that could be described as hot spots (Figure 4). Ambient conditions at CiPEHR are relatively dry, and so we expected that oxidation would be a significant process, but we also suspect that plant-mediated transport could facilitate disproportionately high CH_4 fluxes in wetter years. These hot spots were, with one exception, dominated by graminoid vegetation, primarily *E. vaginatum* (Figure 4). Methane emissions reflect the balance between two counteracting processes: production, where microbial methanogenesis occurs in anaerobic soils, and oxidation where CH_4 is consumed by methanotrophs as it diffuses through aerated soils to the soil surface. Graminoid species are known to be important in soil CH_4 transport and increased surface expression of CH_4 fluxes (King et al., 1998), and CH_4 emissions from plots dominated by graminoid biomass did appear to be influenced by vegetation (Figure 4). Vascular plants can help to bypass oxidation within soils by facilitating rapid transport of belowground CH_4 through root and stem tissues to the soil surface (Davidson et al., 2016; King et al., 1998; McEwing et al., 2015). Since the tussock–forming sedge, *E. vaginatum*, dominates the plant community, plant mediated CH_4 transport could also be important. In 2016, plots with more than 75% graminoid vegetation accounted for 72% of CH_4 emissions from CiPEHR measured that year. In 2017, fewer of these plots were hot spots, and in 2018 none of them were, possibly because of increasing dryness at the site relative to the 2016 growing season. This underscores the importance of accounting for small–scale thaw processes that, depending upon their extent across drier tundra systems, could lead to underestimation of CH_4 emissions. In recent years thermokarst water tracks have become a feature at CiPEHR – in the soil warmed plots but also increasingly across the un–manipulated tundra, and lowland thermokarst is known to be a source of potentially high CH_4 emissions (Olefeldt et al., 2013).

Changes in tundra growing season carbon exchange with soil warming

Models and up–scaling suggest that warmer temperatures and deeper thaw may also stimulate plant growth, potentially offsetting C losses (McGuire et al., 2018), although this vegetation response is likely to be varied across the Arctic and directionality of these trends is far from certain (Abbott et al., 2016; Virkkala et al., 2021). However, more field measurements that represent different landscapes and account for small–scale surface heterogeneity are needed to validate and constrain these, and there are very few full–season CH_4 datasets in warming experiments (Schädel et al., 2018). To estimate the effects of thaw and moisture on the growing season C fluxes at CiPEHR, we calculated the net growing season C budget. Across all thaw depth and moisture groups, CiPEHR was a net C sink during the growing season (Table 3). The effects of soil warming on the C balance depended on a combination of reduced C uptake through GPP and increased CH_4 emission, mediated by moisture. (Table 3).

Over the years measured there were relatively high and low precipitation years, which resulted in commensurate soil moisture conditions (Table 1), and a range of soil C effects. Precipitation in 2016 was relatively high, resulting in shallow WTD and inundated soils in some deeply thawed plots. NEE in Deep Wet plots was reduced relative to Shallow Dry plots, and C storage was further offset by CH_4 emissions in warmed plots by up to 42% from August – September (Figure 5; Table 3). In a drier year like 2017, CH_4 emissions were similar to 2016 (although in 2017 these reflect a full growing season, so overall emissions from May – September likely decreased relative to 2016), while NEE increased in Deep Dry and Deep Wet plots (Figure 5; Table 3). In 2018, with a later start to the growing season due to lingering snow, NEE was slightly suppressed, but due to dry conditions, CH_4 emissions were also reduced by 60–80% of the year before (Figure 5; Table 3).

Permafrost C losses through respiration are predicted to be highest under dry, aerobic conditions that enhance decomposition (Kwon et al., 2019; Lawrence et al., 2015; Natali et al., 2015), and at CiPEHR the proportion of old soil C respired increased 30x relative to wet years (Pegoraro et al., 2020). Under saturated, anaerobic conditions, decomposition processes are slower, and total C losses can be lower than in dry conditions, even accounting for the CO_2–equivalence of CH_4 (Schädel et al., 2016). Nonetheless, our understanding of long term CH_4 production from thawed permafrost is still evolving (Knoblauch et al., 2018). In this study, when accounting for the CO_2–equivalence of CH_4 respired, NEE in Deep Wet plots was consistently most reduced relative to Shallow Dry plots, especially in wetter years. Deep Dry plots exhibited interannual variability in NEE, stemming less from CH_4 respired, and more from the effects of very different growing season lengths and precipitation conditions on plant biomass relative to Shallow Dry plots (Table 1; Table 3).

Shoulder and winter season CH_4 emissions

Upland tundra ecosystems have been shown to emit significant amounts of CH_4 during the shoulder season relative to annual emissions due to incomplete soil freezing (Arndt et al., 2019; Mastepanov et al., 2013; Taylor et al., 2018; Treat et al., 2018; Zona et al., 2016). The zero curtain effect is the observed delay in refreezing of the active layer as a result of the latent heat of unfrozen soil water that maintains soil temperatures near 0˚C (Outcalt et al., 1990; Romanovsky and Osterkamp, 2000). Measurements made at CiPEHR in October–November 2016, show that CH_4 emissions occurred well into the shoulder season even as shallow soil temperatures dropped below 0˚C (Figure 2A; Figure S2). In contrast to the growing season, CH_4 emissions were substantial in drier plots, with emission rates as high 2017 and 2018 growing season, even as soil temperatures declined rapidly. Inundated plots were covered with ice as air temperatures dropped, inhibiting gas diffusion out of soils and limiting fall season emissions.

Winter can be a period of substantial C loss, often offsetting total summer accumulation, and when averaged across treatments, CiPEHR is an annual net source of CO_2 (Webb et al., 2016; Celis et al., 2017; Mauritz et al., 2017; Natali et al., 2019). Methane emissions during winter season may be an additionally significant piece of the annual C budget (Zona et al., 2016). At CiPHER, warmed permafrost soils that are less likely to freeze until late in the shoulder season, and increased snow fall and air warming during the shoulder season may result in taliks, lengthening the zero curtain period and potentially increasing CH_4 and CO_2 respiration (Figure 1C, D; Figure S2). Upland tundra CH_4 emissions measured during winter comprised at least half of annual CH_4 emissions at a nearby (1.3 km) eddy covariance tower (Taylor et al., 2018) in 2016/2017, although there is evidence for winter uptake as well. Estimates of annual greenhouse gas emissions that include winter season are consistently a net C source. Using 2015/2016 winter respiration calculations, estimated annual (October 2015 – September 2016) total C budgets are -102.2 g CO_2-C m^{-2} and -5.2 g CO_2-C–equ from CH_4. Using 2016/2017 winter respiration calculations, estimated annual (October 2016 – September 2017) total C budgets are -96.8 g CO_2-C m^{-2} and -7.6 g CO_2-C–equ from CH_4. Using 2017/2018 winter respiration calculations, estimated annual (October 2017 – September 2018) total C budgets are -133.7 g CO_2-C m^{-2} and 7.0 g CO_2-C–equ from CH_4. This represents a range of 7 to –5.5% of total winter emissions.

Longer–term effects on C balance in tundra systems

Arctic tundra is projected to receive increased annual precipitation both as winter snowfall and annual rainfall (Bring et al., 2016), which is linked with warmer soil temperatures (Iijima et al., 2010), and increased CH_4 emissions (Blanc–Betes et al., 2016;

Neumann et al., 2019; Raz–Yaseef et al. 2017). At CiPEHR, high rainfall years with near surface water table had the highest sustained CH_4 emissions, and in the presence of *E. vaginatum* generated hot spots driving >70% emissions in a very wet year. Therefore, the combination of plant mediated transport and decreased soil gas oxidation may lead to increased emissions under the wettest conditions. In inundated plots, *E. vaginatum* are in decline, and so these CH_4 emissions hot spots may be temporary as the ecosystem transitions, or they may expand depending on the hydrologic trajectory. Over longer time scales, we expect vegetation to shift dependent on the hydrologic changes, possibly to thermokarst wetland, or to a shrub/forest regime (Karlsson et al., 2011). Even in Deep Dry plots we measured increased CH_4 respiration with deeper thaw relative to Shallow Dry, and in the near term these data show dry tundra systems becoming an increasing source of CH_4 in a warming Arctic.

Models suggest that thawed soils could lead to more C uptake because of plant response to warming and CO_2 fertilization (McGuire et al., 2018; Parazoo et al., 2018). Yet field measurements indicate that with transition to wet conditions, C uptake and plant C storage potential in thawing permafrost at CiPEHR is less than models currently estimate (Schädel et al., 2018). It is difficult to determine how the effects of subsidence and rainfall on soil moisture at CiPEHR can be extrapolated to estimate the proportion of dry upland tundra landscape that could transition from a net C sink (D'Imperio et al., 2016; Jørgensen et al., 2014) or low–level source (Euskirchen et al., 2016; Whalen et al., 1991), to a more significant C source because of increasing CH_4 emissions. Long term trends in soil wetting are strongly landscape dependent, where steeper slopes will likely experience more drainage and drying in the long term, and lowland areas and plateaus are likely remain wetter following permafrost thaw (Bring et al., 2016). Large scale changes in soil moisture with thaw are projected to profoundly affect the trajectory and amplitude of future GHG emissions, where wetter soils can lead to a strongly positive GWP by the end of the 21st century due to higher CH_4 emissions in the Arctic (Lawrence et al., 2015).

Acknowledgements

This work was based in part on support provided by the following programs: U.S. Department of Energy, Office of Biological and Environmental Research, Terrestrial Ecosystem Science (TES) Program, Award #DE–SC0006982 and updated with DE–SC0014085 (2015–2018); National Science Foundation Navigating the New Arctic: LTREB: The Arctic Carbon and Climate (ACCLIMATE) Observatory: Tundra Ecosystem Carbon Balance and Old Carbon Loss as a Consequence of Permafrost Degradation, Award #1754839; National Parks Inventory and Monitoring Program; National Science Foundation Bonanza Creek LTER program, Award #1026415; National Science Foundation Office of Polar Programs, Award #1203777. We would like to express our gratitude for assistance from researchers and technicians from the Schuur lab and Bonanza Creek LTER, especially M. Duric, C. So, and G. Frandson, who assisted in these data collections. Data presented in this manuscript are archived at the Bonanza Creek LTER Data Catalog (https://www.lter.uaf.edu/data/data-detail/id/727; doi 10.6073/pasta/7a715a24a19729965d7987aa759e69b9 https://www.lter.uaf.edu/data/data-detail/id/728; doi 10.6073/pasta/2959f51f79d067ce01d2c74a8d5fbb75).

References

Abbott, B.W., Jones, J.B., Schuur, E.A.G., Chapin III, F.S., Bowden, W.B., Bret-Harte, M.S., et al. (2016). Biomass offsets little or none of permafrost carbon release from soils, streams, and wildfire: an expert assessment. *Environmental Research Letters, 11*(3), p.034014.

Andresen C.G., Lara M.J., Tweedie C.E., & Lougheed V.L. (2017). Rising plant–mediated methane emissions from arctic wetlands. *Global Change Biology*, *23*(3), 1128–1139.

Arndt, K.A., Oechel, W.C., Goodrich, J.P., Bailey, B.A., Kalhori, A., Hashemi, J., et al. (2019). Sensitivity of methane emissions to later soil freezing in arctic tundra ecosystems. *Journal of Geophysical Research: Biogeosciences*, *124*(8), 2595–2609.

Belshe, E. F., Schuur, E. A. G. & Bolker, B. M. (2013)a. Tundra ecosystems observed to be CO_2 sources due to differential amplification of the carbon cycle. *Ecology Letters*, *16*, 1307–1315.

Belshe, E. F., Schuur, E. A. G. & Grosse, G. (2013)b. Quantification of upland thermokarst features with high resolution remote sensing. *Environmental Research Letters*, *8*(3), 035016.

Blanc–Betes, E., Welker, J. M., Sturchio, N. C., Chanton, J. P. & Gonzalez–Meler, M. A. (2016). Winter precipitation and snow accumulation drive the methane sink or source strength of Arctic tussock tundra. *Global Change Biology*, *22*(8), 2818–2833.

Bring, A., Fedorova, I., Dibike, Y., Hinzman, L., Mård, J., Mernild, S.H., et al. (2016). Arctic terrestrial hydrology: A synthesis of processes, regional effects, and research challenges. *Journal of Geophysical Research: Biogeosciences, 121*(3), 621 – 649.

Celis G., Mauritz M., Bracho R., Salmon, V., Webb, E.E., Hutchings, J., et al. (2017). Tundra is a consistent source of CO_2 at a site with progressive permafrost thaw during 6 years of chamber and eddy covariance measurements. *Journal of Geophysical Research: Biogeosciences, 122*(6), 1471–1485.

Chowdhury, T. R., Herndon, E.M., Phelps, T.J., Elias, W.A., Gu, B., Liang, L., et al. (2015). Stoichiometry and temperature sensitivity of methanogenesis and CO_2 production from saturated polygonal tundra in Barrow, Alaska. *Global Change Biology*, *21*(2), 722–737.

D'Imperio, L., Nielsen, C. S., Westergaard–Nielsen, A., Michelsen, A. & Elberling, B. (2016). Methane oxidation in contrasting soil types: responses to experimental warming with implication for landscape–integrated CH_4 budget. *Global Change Biology*, *23*(2), 966–976.

Davidson, S. J., Sloan, V.L., Phoenix, G.K., Wagner, R., Fisher, J.P., Oechel, W.C., & Zona, D. (2016) Vegetation type dominates the spatial variability in CH_4 emissions across multiple Arctic tundra landscapes. *Ecosystems*, *19*(16), 1116–1132.

Dean, J. F., Middleburg, J.J., Röckmann, T., Aerts, R., Blauw, L.G., Egger, M., et al. (2018). Methane feedbacks to the global climate system in a warmer world. *Reviews of Geophysics, 56*(1), 207–250.

Euskirchen, E. S., Bret–Harte, M. S., Shaver, G. R., Edgar, C. W. & Romanovsky, V. E. (2016). Long–term release of carbon dioxide from Arctic tundra ecosystems in Alaska. *Ecosystems*, *20*(5), 960–974.

Hugelius, G., Strauss, J., Zubrzycki, S., Harden, J.W., Schuur, E.A.G., Ping, C.–L., et al. (2014). Estimated stocks of circumpolar permafrost carbon with quantified uncertainty ranges and identified data gaps. *Biogeosciences*, *11*(23), 6573–6593.

Humphrey, V., Berg, A., Ciais, P., Gentine, P., Jung, M., Reichstein, M., et al. (2021). Soil moisture-atmosphere feedback dominates land carbon uptake variability. *Nature, 592*(7852), 65-69.

Iijima, Y., Fedorov, A.N., Park, H., Suzuki, K., Yabuki, H., Maximov, T.C., & Ohata, T. (2010) Abrupt increases in soil temperatures following increased precipitation in a permafrost region, central Lena River basin, Russia. *Permafrost and Periglacial Processes*, *21*(1), 30–41.

Jørgensen, C.J., Lund Johansen, K. M., Westergaard–Nielsen, A. & Elberling, B. (2014). Net regional methane sink in High Arctic soils of northeast Greenland. *Nature Geoscience*, *8*(1), 20–23.

Karlsson, J.M., Bring, A., Peterson, G.D., Gordon, L.J., & Destouni, G. (2011). Opportunities and limitations to detect climate–related regime shifts in inland Arctic ecosystems through eco–hydrological monitoring. *Environmental Research Letters*, *6*(1), 014015.

King, J. Y., Reeburgh, W. S. & Regli, S. K. (1998). Methane emission and transport by arctic sedges in Alaska: Results of a vegetation removal experiment. *Journal of Geophysical Research*, *103*(D22), 29,083–29,092.

Knoblauch, C., Beer, C., Liebner, S., Grigoriev, M.N., & Pfeiffer, E–M. (2018). Methane production as key to the greenhouse gas budget of thawing permafrost. *Nature Climate Change*, *8*, 309–312.

Koven, C. D., Ringeval, B., Friedlingstein, P., Ciais, P., Cadule, P., Khvorostyanov, D., et al. (2011). Permafrost carbon–climate feedbacks accelerate global warming. *Proceedings of the National Academy of Sciences*, *108*(36), 14,769–14,774.

Koven, C. D., Schuur, E.A.G, Schädel, C., Bohn, T.J., Burke, E.J., Chen, G., et al. (2015). A simplified, data–constrained approach to estimate the permafrost carbon–climate feedback. *Philosophical Transactions A, 373*, 20140423.

Kwon, M. J., Natali, S.M., Hicks Pries, C.E., Schuur, E.A.G., Steinhof, A., Crummer, G., et al. (2019). Drainage enhances modern soil carbon contribution but reduces old soil carbon contribution to ecosystem respiration in tundra ecosystems. *Global Change Biology*, *25*(4), 1315–1325.

Lawrence, D. M., Koven, C. D., Swenson, S. C., Riley, W. J. & Slater, A. G. (2015). Permafrost thaw and resulting soil moisture changes regulate projected high–latitude CO_2 and CH_4 emissions. *Environmental Research Letters, 10*(9), 094011.

Lee, H., Schuur, E. A. G. & Vogel, J. G. (2010). Soil CO_2 production in upland tundra where permafrost is thawing. *Journal of Geophysical Research*, *115*(G1), G01009.

Lique, C., Holland, M. M., Dibike, Y. B., Lawrence, D. M. & Screen, J. A. (2016). Modeling the Arctic freshwater system and its integration in the global system: Lessons learned and future challenges. *Journal of Geophysical Research: Biogeosciences, 121*, 540–566.

Mastepanov, M., Sigsgaard, C., Tagesson, T., Ström, L., Tamstorf, M.P., Lund, M., et al. (2013). Revisiting factors controlling methane emissions from high–Arctic tundra. *Biogeosciences, 10*(7), 5139–5158.

Mauritz, M., Bracho, R., Celis, G., Hutchings, J., Natali, S.M., Pegoraro, E., et al. (2017). Nonlinear CO_2 flux response to 7 years of experimentally induced permafrost thaw. *Global Change Biology*, *23*(9), 3646–3666.

Mauritz, M., Celis, G., Ebert, C., Hutchings, J., Ledman, J., Natali, S.M., et al. (2019). Using stable carbon isotopes of seasonal ecosystem respiration to determine permafrost carbon loss. *Journal of Geophysical Research: Biogeosciences*, *124*, 034014.

McEwing, K. R., Fisher, J. P. & Zona, D. (2015). Environmental and vegetation controls on the spatial variability of CH_4 emission from wet–sedge and tussock tundra ecosystems in the Arctic. *Plant Soil*, *388*(1–2), 37–52.

McGuire, A. D., Lawrence, D.M., Koven, C., Clein, J.S., Burke, E., Chen, G., et al. (2018). Dependence of the evolution of carbon dynamics in the northern permafrost region on the trajectory of climate change. *Proceedings of the National Academy of Sciences*, *115*(15), 3882–3887.

Natali, S. M., Schuur, E.A.G., Trucco, C., Hicks Pries, C.E., Crummer, K.G., & Baron Lopez, A.F. (2011). Effects of experimental warming of air, soil and permafrost on carbon balance in Alaskan tundra. *Global Change Biology*, *17*(3), 1394–1407.

Natali, S. M., Schuur, E. A. G. & Rubin, R. L. (2012). Increased plant productivity in Alaskan tundra as a result of experimental warming of soil and permafrost. *Journal of Ecology*, *100*(2), 488–498.

Natali, S. M., Schuur, E. A. G., Webb, E. E., Hicks Pries, C. E. & Crummer, K. G. (2014). Permafrost degradation stimulates carbon loss from experimentally warmed tundra. *Ecology*, *95*(3), 602–608.

Natali, S. M., Schuur, E. A. G., Mauritz, M., Schade, J.D., Celis, G., Crummer, K. G., et al. (2015). Permafrost thaw and soil moisture driving CO_2 and CH_4 release from upland tundra. *Journal of Geophysical Research: Biogeosciences, 120,* 525–537.

Natali, S.M., Watts, J.D., Rogers, B.M., Potter, S., Ludwig, S.M., Selbmann, A–K., et al. (2019). Large loss of CO_2 in winter observed across the northern permafrost region. *Nature Climate Change, 9*, 852–857.

Nauta, A. L., Heijmans, M.M.P.D., Blok, D., Limpens, J., Elberling, B., Gallagher, A., et al. (2015). Permafrost collapse after shrub removal shifts tundra ecosystem to a methane source. *Nature Climate Change*, *5*(1), 67–70.

Neubauer, S. C. & Megonigal, J. P. (2019). Moving beyond global warming potentials to quantify the climatic role of ecosystems. *Ecosystems*, *18*, 1000–1013.

Neumann, R.B., Moorberg, C.J., Lundquist, J.D., Turner, J.C., Waldrop, M.P., McFarland J.W., et al. (2019). Warming effects of spring rainfall increase methane emissions from thawing permafrost. *Geophysical Research Letters*, *46*(3), 1393–1401.

Olefeldt, D., Turetsky, M. R., Crill, P. M. & McGuire, A. D. (2013). Environmental and physical controls on northern terrestrial methane emissions across permafrost zones. *Global Change Biology*, *19*(2), 589–603.

Olefeldt, D., Goswami, S., Grosse, G., Hayes, D., Hugelius, G., Kuhry, P., et al. (2016). Circumpolar distribution and carbon storage of thermokarst landscapes. *Nature Communications*, *7*, 1–11.

Osterkamp, T. E. & Romanovsky, V. E. (1999). Evidence for warming and thawing of discontinuous permafrost in Alaska. *Permafrost and Periglacial Processes*, *10*, 17–37.

Osterkamp, T. E., Jorgenson, M.T., Schuur, E.A.G., Shur, Y.L., Kanevskiy, M.Z., Vogel, J.G., & Tumskoy, V.E. (2009). Physical and ecological changes associated with warming permafrost and thermokarst in Interior Alaska. *Permafrost and Periglacial Processes*, *20*(3), 235–256.

Outcalt, S. I., Nelson, F. E. & Hinkel, K. M. (1990). The zero–curtain effect: Heat and mass transfer across an isothermal region in freezing soil. *Water Resources Research*, *26*(7), 1509–1516.

Overland, J.E., Hanna, E., Hanssen–Bauer, I., Kim, J., Walsh, J.E., Wang, M., et al. (2018). Surface air temperature. *2018 Arctic Report Card.*

Parazoo, N. C., Koven, C. D., Lawrence, D. M., Romanovsky, V. & Miller, C. E. (2018). Detecting the permafrost carbon feedback: talik formation and increased cold–season respiration as precursors to sink–to–source transitions. *The Cryosphere*, *12*(1), 123–144.

Pinheiro, J. C., & Bates, D. M. (2000). Extending the basic linear mixed–effects model. In *Mixed–effects models in S and S–PLUS* (pp. 201–270). New York: Springer–Verlag.

Pinheiro J., Bates D., DebRoy S., Sarkar D., & R Core Team. (2017). *nlme: Linear and Nonlinear Mixed Effects Models*. R package version 3.1–131, https://CRAN.R–project.org/package=nlme.

Plaza, C., Pegoraro, E., Bracho, R., Celis, G., Crummer, K.G., Hutchings, J.A., et al. (2019). Direct observation of permafrost degradation and rapid soil carbon loss in tundra. *Nature Geoscience*, *12*, 627 – 631.

Pegoraro, E.F., Mauritz, M., Ogle, K., Ebert, C.H., Schuur, E.A.G. (2020). Lower soil moisture ad deep soil temperatures in thermokarst features increase old soil carbon loss after 10 years of experimental permafrost warming. *Global Change Biology*, *27*(6), 1293–1308.

Preuss, I., Knoblauch, C., Gebert, J., Pfeiffer, E.–M. (2013). Improved quantification of microbial CH4 oxidation efficiency in arctic wetland soils using carbon isotope fractionation. *Biogeosciences, 10*, 2539–2552.

Raz–Yaseef, N., Torn, M.S., Wu, Y., Billesbach, D.P., Liljedahl, A.K., Kneafsey, T.J., et al. (2017). Large CO_2 and CH_4 emissions from polygonal tundra during spring thaw in northern Alaska. *Geophysical Research Letters, 44*(1), 504–513.

Rodenhizer, H., Ledman, J., Mauritz, M., Natali, S.M., Pegoraro, E., Plaza, C., Romano, E., Schädel, C., Taylor, M., Schuur, E. (2020). Carbon thaw rate doubles when accounting for subsidence in a permafrost warming experiment. *Journal of Geophysical Research: Biogeosciences*, *125*, e2019JG005528.

Romanovsky, V. E. & Osterkamp, T. E. (2000). Effects of unfrozen water on heat and mass transport processes in the active layer and permafrost. *Permafrost and Periglacial Processes*, *11*, 219–239.

Salmon, V. G., Soucy, P., Mauritz, M., Celis, G., Natali, S.M., Mack, M.C., & Schuur, E.A.G. (2016). Nitrogen availability increases in a tundra ecosystem during five years of experimental permafrost thaw. *Global Change Biology*, *22*(5), 1927–1941.

Schädel, C., Bader, M.F.K., Schuur, E.A.G., Biasi, C., Bracho, R., Čapek, P., et al. (2016). Potential carbon emissions dominated by carbon dioxide from thawed permafrost soils. *Nature Climate Change*, *6*(10), 950–953.

Schädel, C., Koven, C.D., Lawrence, D.M., Celis, G., Garnello, A.J., Hutchings, J., et al. (2018). Divergent patterns of experimental and model–derived permafrost ecosystem carbon dynamics in response to Arctic warming. *Environmental Research Letters, 13*(10), 105002.

Schaefer, K., Zhang, T., Bruhwiler, L. & Barrett, A. P. (2011). Amount and timing of permafrost carbon release in response to climate warming. *Tellus B, 63B*, 165–180.

Schuur, E. A. G., Crummer, K. G., Vogel, J. G. & Mack, M. C. (2007). Plant species composition and productivity following permafrost thaw and thermokarst in Alaskan tundra. *Ecosystems*, *10*(2), 280–292.

Schuur, E. A. G., Vogel, J.G., Crummer, K.G., Lee, H., Sickman, J.O., & Osterkamp, T.E. (2009). The effect of permafrost thaw on old carbon release and net carbon exchange from tundra. *Nature, 459*(556–559), 556–559.

Schuur, E. A. G., McGuire, A.D., Schädel, C., Grosse, G., Harden, J.W., Hayes, D.J., et al. (2015). Climate change and the permafrost carbon feedback. *Nature*, *520*(7546), 171–179.

Schuur, E. A. G., & Mack, M. C. (2018). Ecological response to permafrost thaw and consequences for local and global ecosystem services. *Annual Review of Ecology, Evolution, and Systematics*, *49*(49), 279–301.

Schuur, E. A. G., A. D. McGuire, V. Romanovsky, C. Schädel, and M. Mack, 2018: Chapter 11: Arctic and boreal carbon. In Second State of the Carbon Cycle Report (SOCCR2): A Sustained Assessment Report [Cavallaro, N., G. Shrestha, R. Birdsey, M. A. Mayes, R. G. Najjar, S. C. Reed, P. Romero–Lankao, and Z. Zhu (eds.)]. U.S. Global

Change Research Program, Washington, DC, USA, pp. 428–468, https://doi.org/10.7930/SOCCR2.2018.Ch11.

Sturtevant, C. S., Oechel, W. C., Zona, D., Kim, Y. & Emerson, C. E. (2012). Soil moisture control over autumn season methane flux, Arctic Coastal Plain of Alaska. *Biogeosciences*, *9*, 1423–1440.

Tarnocai, C., Canadell, J.G., Schuur, E.A.G., Kuhry, P., Mazhitova, G., & Zimov, S. (2009). Soil organic carbon pools in the northern circumpolar permafrost region. *Global Biogeochemical Cycles*, *23*, GB2023.

Taylor, M., Schuur, E.A.G.; Mauritz, M. Pegoraro, E. F.; Salmon, V. G.; Natali, S.M. (2017). *Eight Mile Lake Research Watershed, Carbon in Permafrost Experimental Heating Research (CiPEHR): Aboveground plant biomass, 2009–2017*, Bonanza Creek LTER – University of Alaska Fairbanks.

Taylor, M. A., Celis, G., Ledman, J. D., Bracho, R. & Schuur, E. A. G. (2018). Methane efflux measured by eddy covariance in Alaskan upland tundra undergoing permafrost degradation. *Journal of Geophysical Research: Biogeosciences*, *123*, 2695–2710.

Treat, C.C., Bloom, A.A., & Marushchak, M. E. (2018). Nongrowing season methane emissions – a significant component of annual emissions across northern ecosystems. *Global Change Biology*, *24*(8), 3331–3343.

Vaughn, L. J. S., Conrad, M. E., Bill, M. & Torn, M. S. (2016). Isotopic insights into methane production, oxidation, and emissions in Arctic polygon tundra. *Global Change Biology*, *22*(10), 3487–3502

Virkkala, A-M, Aalto, J., Rogers, B.M., Tagesson, T., Treat, C.C., Natali, S.M., et al. (2021). Statistical upscaling of ecosystem CO_2 fluxes across the terrestrial tundra and boreal domain: regional patterns and uncertainties. *Global Change Biology*.

Vogel, J., Schuur, E. A. G., Trucco, C. & Lee, H. (2009). Response of CO_2 exchange in a tussock tundra ecosystem to permafrost thaw and thermokarst development. *Journal of Geophysical Research***,** *114*, G04018.

Voigt, C., Lamprecht, R.E., Marushchak, M., Lind, S.E., Novakovskiy, A., Aurela, M., et al. (2017). Warming of subarctic tundra increases emissions of all three important greenhouse gases – carbon dioxide, methane, and nitrous oxide. *Global Change Biology*, *23*(8), 3121 – 3138.

Voigt, C., Marushchak, M.E., Mastepanov, M., Lamprecht, R.E., Christensen, T.R., Dorodnikov, M., et al. (2019). Ecosystem carbon response of Arctic peatlands to simulated permafrost thaw. *Global Change Biology*, *25*(5), 1746 – 1764.

von Fischer, J. C., Rhew, R. C., Ames, G. M., Fosdick, B. K. & von Fischer, P. E. (2010). Vegetation height and other controls of spatial variability in methane emissions from the Arctic coastal tundra at Barrow, Alaska. *Journal of Geophysical Research*, *115*, 16645.

Walker, D. A., Raynolds, M.K., Daniëls, F.J.A., Einarsson, E., Elvebakk, A., Gould, W.A., et al. (2005). The Circumpolar Arctic vegetation map. *Journal of Vegetation Science*, *16*(3), 267–282.

Walvoord, M.A. and Kurylyk, B.L. (2016). Hydrologic impacts of thawing permafrost – A review. *Vadose Zone Journal*, *15*(6), 1–20.

Webb, E. E., Schuur, E.A.G., Natali, S.M., Oken, K.L., Bracho, R., Krapek, J.P., et al. (2016). Increased wintertime CO_2 loss as a result of sustained tundra warming. *Journal of Geophysical Research: Biogeosciences*, *121*, 249–265.

Whalen, S. C., Reeburgh, W. S. & Kizer, K. S. (1991). Methane consumption and emission by taiga. *Global Biogeochemical Cycles*, *5*(3), 261–273.

Whalen, S.C. (2005). Biogeochemistry of methane exchange between natural wetlands and the atmosphere. *Environmental Engineering Science, 22*(1) 73–94.

Wrona, F. J. Johansson, M., Culp, J.M., Jenkins, A., Mård, J., Myers–Smith, I.H., et al. (2016). Transitions in Arctic ecosystems: Ecological implications of a changing hydrological regime. *Journal of Geophysical Research: Biogeosciences, 121*, 650–674.

Zona, D., Oechel, W.C., Kochendorfer, J., Paw U, K.T., Salyuk, A.N., Olivas, P.C., et al. (2009). Methane fluxes during the initiation of a large–scale water table manipulation experiment in the Alaskan Arctic tundra. *Global Biogeochemical Cycles, 23*, GB2013

Zona, D., Gioli, B., Commane, R., Lindaas, J., Wofsy, S.C., Miller, C.E., et al. (2016). Cold season emissions dominate the Arctic tundra methane budget. *Proceedings of the National Academy of Sciences*, *113*(1), 40–45.

Zuur, A. F., Ieno, E. N., Walker, N., Saveliev, A. A., & Smith, G. M. (2009). *Mixed effects models and extensions in ecology with R*. New York: Springer.

Figure Captions

Figure 1. Environmental variables measured during the growing seasons in 2016, 2017, and 2018. Mean air temperature (circles) and cumulative weekly precipitation (bars) are plotted in A) with standard error bars. Mean weekly depth to water table (closed circles) and thaw depth (open circles) are plotted by B) Shallow Dry, C) Deep Dry, and D) Deep Wet groupings. Dashed line at 0 cm marks the soil surface. For details about number of measurements made please see Table 1.

Figure 2. Mean daily CH_4 fluxes (circles) during A) the 2016 end of summer and shoulder season fluxes and B) 2017 and C) 2018 growing season fluxes for each plot sampled. Note different y-axis scales for Deep Wet plots.

Figure 3. Responses of daily CH_4 fluxes plotted on a log scale to mean weekly thaw depths (panels A and B) and mean deep soil temperatures (panels C and D) plotted by data groupings in 2017 and 2018.

Figure 4. Daily CH_4 fluxes during 2016 – 2018 growing seasons plotted against mean weekly WTD. Top panels are plots with >75% graminoid biomass, and bottom panels are plots with <75% graminoid biomass. Note the different y-axis scales.

Figure 5. Mean cumulative C emissions are plotted for A) Shallow Dry (N = 22) and B) Deep Dry (n = 8), and C) Deep Wet (n = 12) growing seasons. In 2016, NEE spans May 1 - November 31st, while CH_4 measurements span August - November 31st. NEE and CH_4 measurements span the growing season, May 1st – September 30th, in 2017 and

2018. S.E. is standard error. Total net ecosystem exchange of g CO_2-C (top panels) and CO_2–equivalent calculated from CH_4 fluxes expressed in g CO_2-C m^{-2} (bottom panels) are averaged from all plots measured between groups and plotted with standard error bars. Positive values reflect a net C sink and negative values are a net source.

Figure 1.

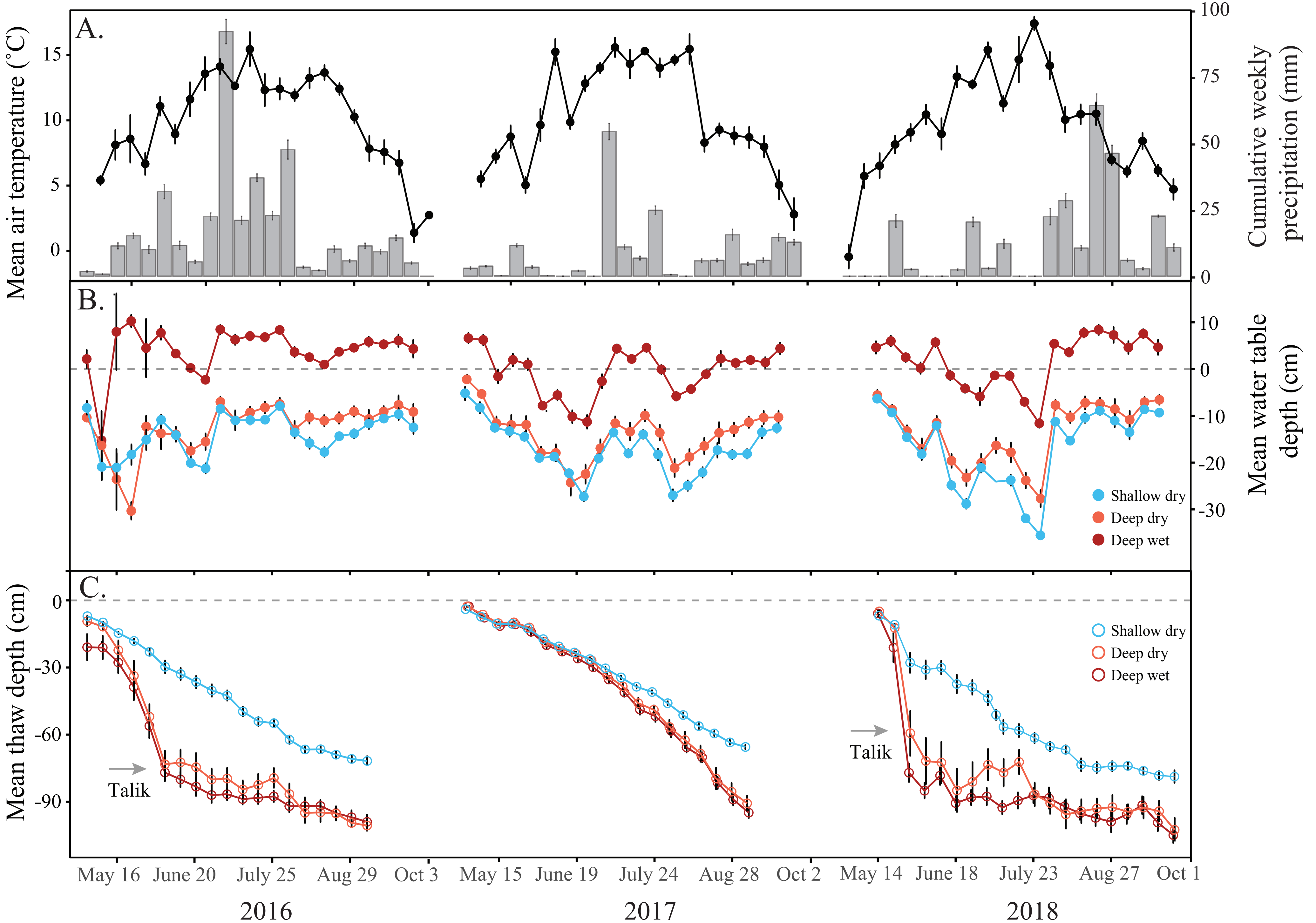

A.
B.
C.
Mean air temperature (°C)
Cumulative weekly precipitation (mm)
Mean water table depth (cm)
Mean thaw depth (cm)
Shallow dry
Deep dry
Deep wet
Talik
Talik
May 16
June 20
July 25
Aug 29
Oct 3
May 15
June 19
July 24
Aug 28
Oct 2
May 14
June 18
July 23
Aug 27
Oct 1
2016
2017
2018

Figure 2.

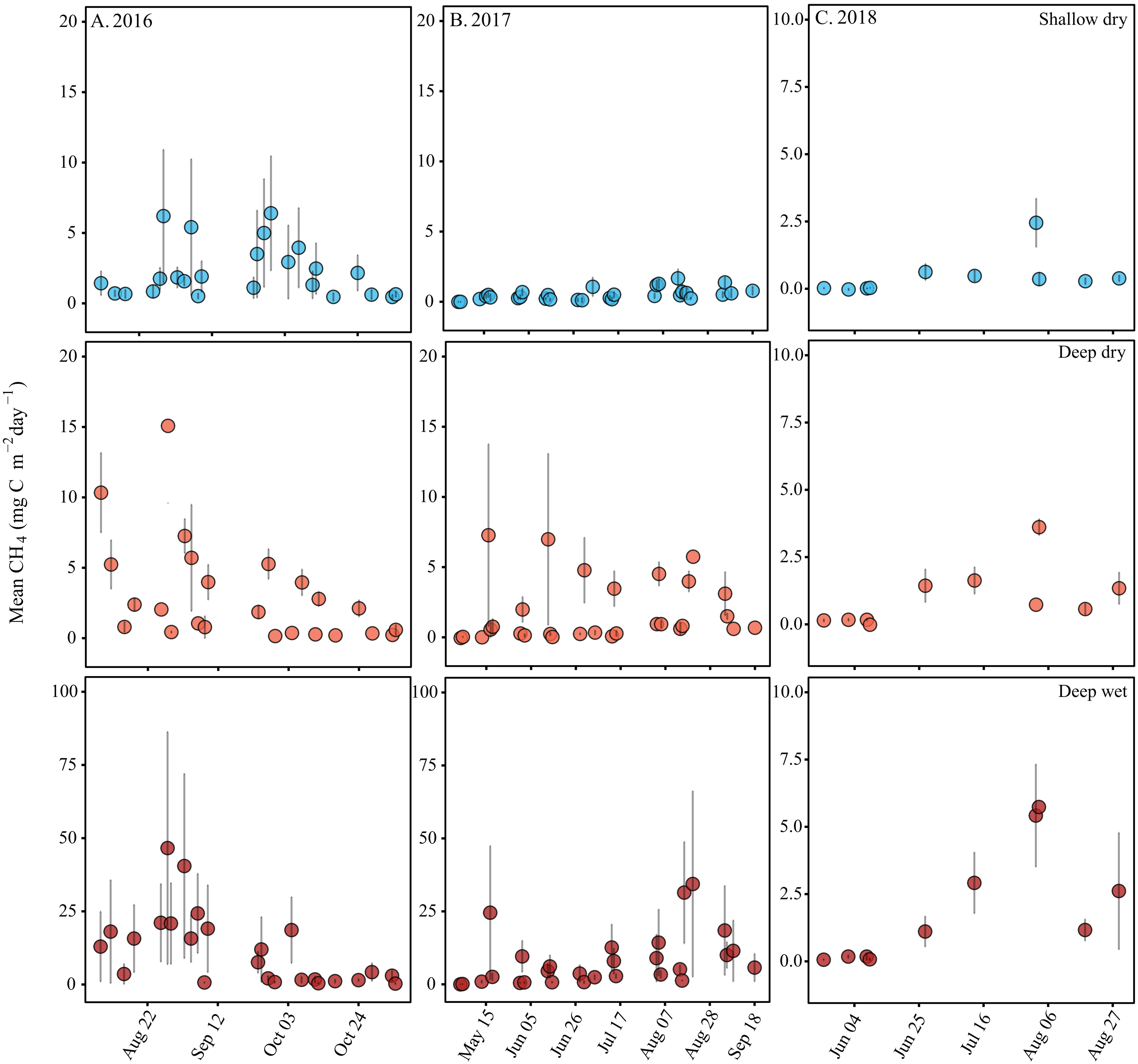

A. 2016
B. 2017
C. 2018
Shallow dry
Deep dry
Deep wet
Mean CH_4 (mg C m^{-2} day^{-1})
Aug 22
Sep 12
Oct 03
Oct 24
May 15
Jun 05
Jun 26
Jul 17
Aug 07
Aug 28
Sep 18
Jun 04
Jun 25
Jul 16
Aug 06
Aug 27

Figure 3.

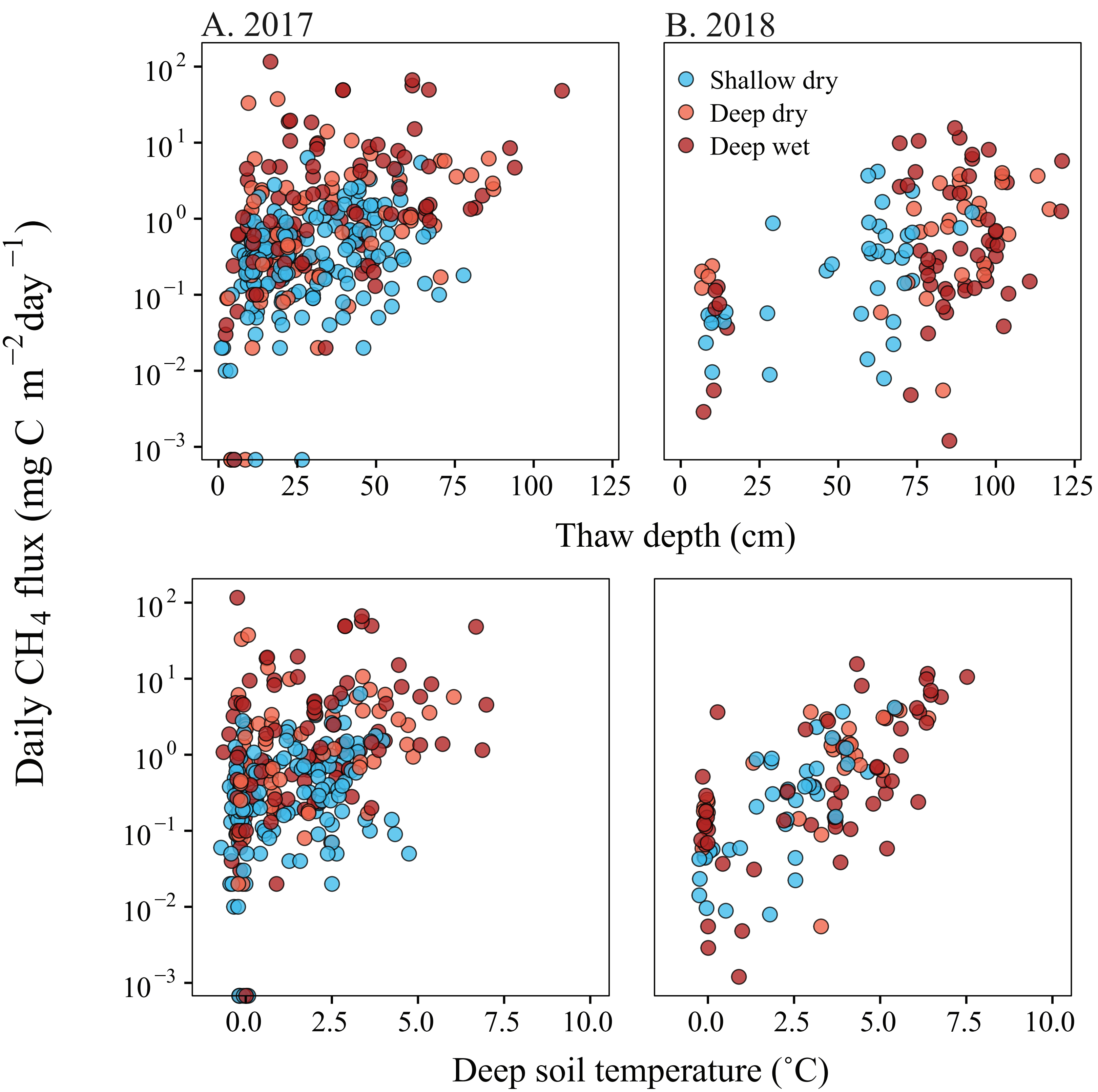

A. 2017
B. 2018
Shallow dry
Deep dry
Deep wet
Daily CH4 flux (mg C m−2day−1)
Thaw depth (cm)
Deep soil temperature (˚C)
10^2
10^1
10^0
10^−1
10^−2
10^−3
0
25
50
75
100
125
0.0
2.5
5.0
7.5
10.0

Figure 4.

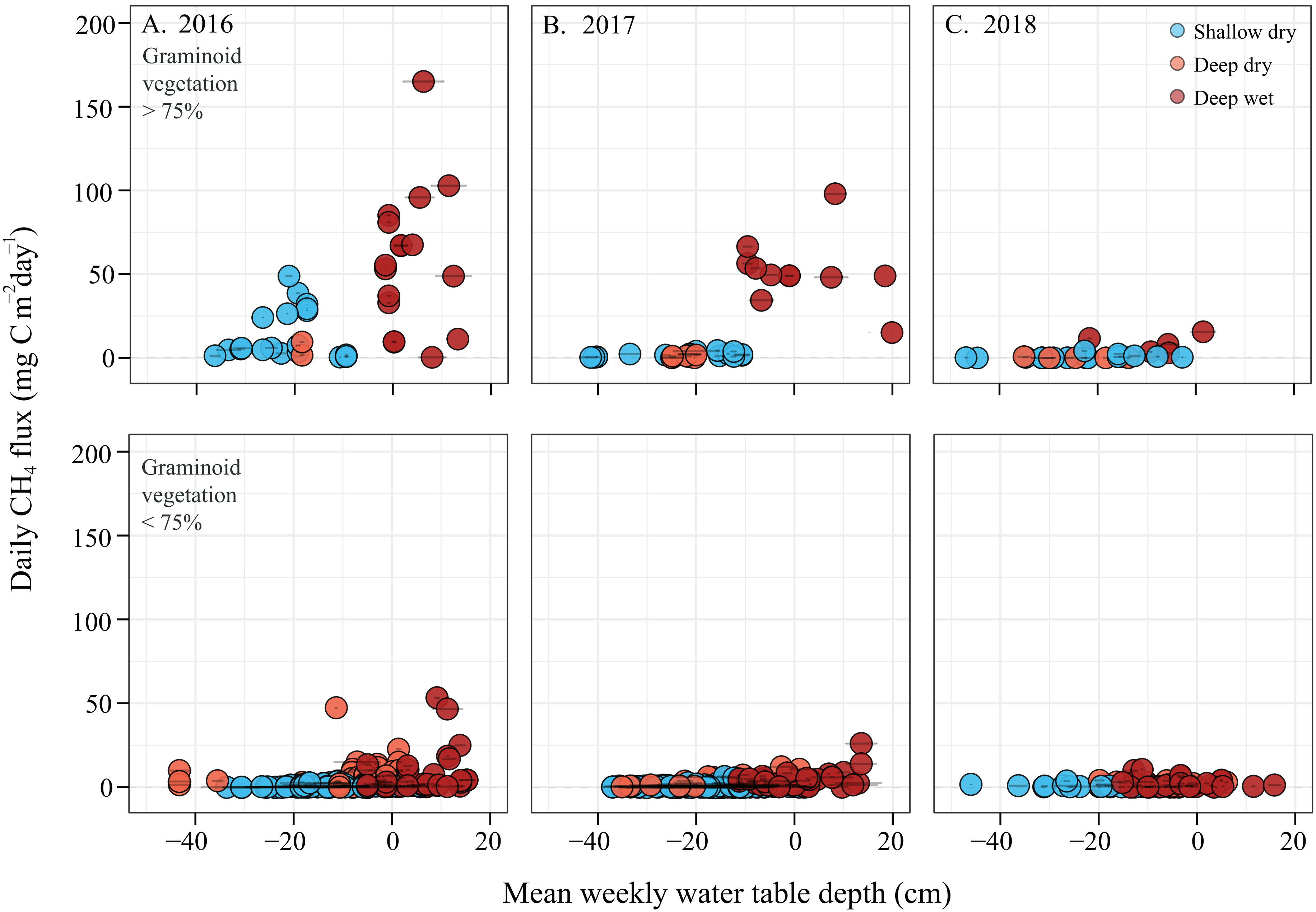

A. 2016
B. 2017
C. 2018
Graminoid vegetation > 75%
Graminoid vegetation < 75%
Shallow dry
Deep dry
Deep wet
Daily CH_4 flux (mg C $m^{-2}day^{-1}$)
Mean weekly water table depth (cm)
200
150
100
50
0
−40
−20
0
20

Figure 5.

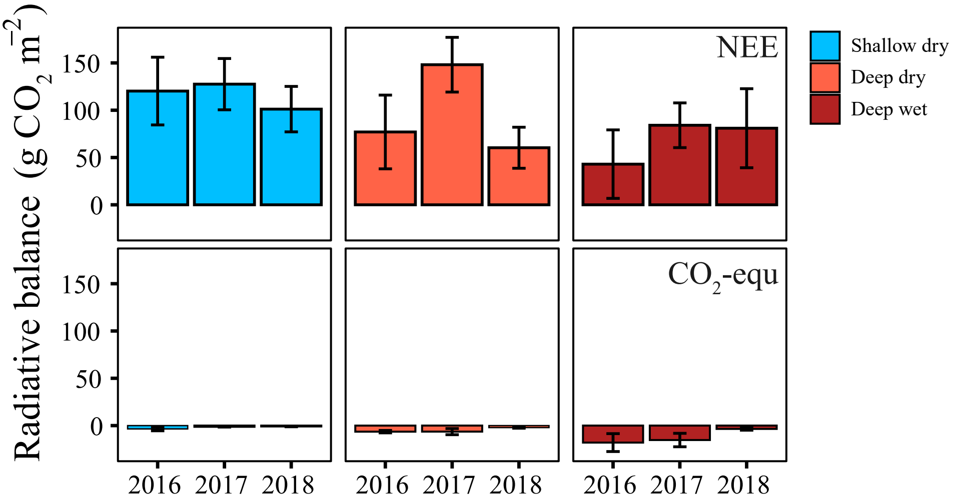

Radiative balance (g CO_2 m^{-2})
150
100
50
0
NEE
CO_2-equ
2016
2017
2018
Shallow dry
Deep dry
Deep wet

Table 1.
Environmental variables measured at the site during the growing season (May 1 - September 30th)
Standard error is reported as s.e.

Variable	Season	2016			2017		
Air temperature ˚C	growing season	10.3			10.4		
	s.e.	0.3			0.4		
	N	153			153		
Sum precipitation	Sum growing season	392.4			187.2		
(mm)	s.e.	0.4			0.3		
	N	153			153		
		Shallow dry	Deep dry	Deep wet	Shallow dry	Deep dry	Deep wet
Shallow soils ˚C	Mean growing	5.7	5.8	6.5	5.3	5.3	5.5
(5 - 10 cm)	s.e.	0.1	0.1	0.1	0.1	0.1	0.1
	N	3366	1224	1836	3366	1224	1836
Deep soils ˚C	growing season	2.0	3.0	3.4	1.4	1.8	2.0
(20 - 40 cm)	s.e.	0.0	0.1	0.1	0.0	0.1	0.0
	N	3366	1224	1836	3366	1224	1836
WTD (cm)	growing season	13.7	10.6	-3.2	18.7	13.3	0.1
	s.e.	0.2	0.4	0.3	0.3	0.5	0.3
	N	2024	736	1104	1438	522	782
ALT (cm)	Max growing season	78.9	108.5	120.2	68.4	99.8	102.9
	s.e.	3.3	4.7	4.2	1.4	5.4	3.3
	N	8	12	22	8	12	22

2018		
9.7		
0.4		
153		
275.4		
0.4		
153		
Shallow dry	Deep dry	Deep wet
4.9	5.0	5.6
0.1	0.1	0.1
3366	1224	1836
1.7	2.4	2.4
0.0	0.1	0.1
3366	1224	1836
19.0	14.7	0.2
0.3	0.5	0.3
1892	688	1032
84.9	113.9	113.0
3.3	4.1	3.1
8	12	22

Table 2.

A) Growing season (May - September) 2017 CH_4 flux linear mixed effects model

Backward stepwise model selection was used to obtain final model.

Full model: WTD, thaw depth, DST, random effect (plot)

Response variable	Final model	Coefficient	2.5 % CI	97.5% CI	R^2 marginal	R^2conditional
Cumulative weekly CH_4 emission (mg C-CH_4 m^{-2} $week^{-1}$)	Intercept	1.94	1.70	2.19	0.13	0.64
	Thaw depth	0.77	0.53	1.02		
	WTD	0.36	0.12	0.61		

B) Growing season (May - August) 2018 CH_4 flux linear mixed effects model

Backward stepwise model selection was used to obtain final model.

Full model: WTD, thaw depth, DST, random effect (plot)

Response variable	Final model	Coefficient	2.5 % CI	97.5% CI	R^2 marginal	R^2conditional
Cumulative weekly $CH_{4emission}$ (mg C-CH_4 m^{-2} $week^{-1}$)	Intercept	1.61	1.27	1.97	0.42	0.79
	DST	1.86	1.64	2.10		
	Thaw depth	-0.52	-0.93	-0.09		
	DST x Thaw depth	-1.23	-1.72	-0.74		

WTD is mean weekly water tale depth (cm), thaw depth is mean weekly thaw depth (cm), DST is mean weekly deep soil temperature (20 - 40 cm) ˚C.

Table 3. Cumulative net ecosystem exchange (NEE), CH_4 emissions, and CO_2-equivalent CH_4 measur
In 2016, NEE spans May 1 - November 31st, while CH_4 measurements span August - November 31st.
NEE and CH_4 measurements span the growing season, May 1st - September 30th, in 2017 and 2018. S

Group	Year	NEE (g CO_2-C m^{-2})	N	S.E.	CH_4 (mg CH_4-C m^{-2})	N
Shallow dry	2016	120.2	9630	35.8	-215.7	187
Deep dry	2016	77.0	7442	39.0	-392.3	90
Deep wet	2016	43.0	7498	36.2	-1099.4	103
Shallow dry	2017	127.5	9347	27.1	-78.6	234
Deep dry	2017	148.1	7344	28.9	-390.5	85
Deep wet	2017	84.1	7344	23.6	-934.3	130
Shallow dry	2018	101.1	9347	24.0	-55.6	50
Deep dry	2018	60.3	7344	21.7	-129.8	35
Deep wet	2018	81.0	7344	41.8	-216.1	35

Group	Year	CO_2-equivalent (g CO_2 - C m^{-2})	N	S.E.	NEE % decrease
Shallow dry	2016	-3.5	187	2.0	2.9
Deep dry	2016	-6.4	90	1.3	8.3
Deep wet	2016	-18.0	103	9.5	41.8
Shallow dry	2017	-1.3	234	0.3	1.0
Deep dry	2017	-6.4	85	3.3	4.3
Deep wet	2017	-15.3	130	7.1	18.2
Shallow dry	2018	-0.9	50	0.3	0.9
Deep dry	2018	-2.1	35	0.6	3.5
Deep wet	2018	-3.5	35	1.4	4.4

ed across 2016 - 2018.

.E. is standard error.

S.E.
120.1
78.5
578.2
17.3
198.6
433.6
20.7
39.3
82.4